

# Contactless Excitation and Readout of Passive Sensing Elements Made by Miniaturized Mechanical Resonators

M. Baù, V. Ferrari, D. Marioli, E. Sardini, M. Serpelloni, A. Taroni  
Dept. of Electronics for Automation  
University of Brescia  
Brescia, Italy  
[marco.bau@ing.unibs.it](mailto:marco.bau@ing.unibs.it)

**Abstract**— Mechanical resonance has been contactless excited and detected in conductive nonmagnetic structures to be used as sensors without the need for external magnets, or electrical connections to the structure to supply current lines. An external coil generates a magnetic field at frequency  $f$  that induces eddy currents in the structure. The interaction between the eddy currents and the magnetic field itself causes Lorentz forces at frequency  $2f$  that can set the structure into resonance. An additional dual-coil arrangement applies and senses a probing magnetic field at higher frequency and exploits it to measure the resonator vibrations. The principle was tested on millimeter-size metallic beams, obtaining operation distances in the order of 1 cm and values of the resonant frequencies in agreement with measurements taken by an optical system. The resulting resonators can be used as passive sensing elements for a variety of quantities, being especially attractive for harsh and inaccessible environments.

## I. INTRODUCTION

The availability of passive sensors that can be interrogated contactless is attractive for operation in harsh environments incompatible with active electronics, e.g. at high temperature, and/or in applications that do not allow for cabled solutions, e.g. for in-package or in-body measurements. Mechanical resonator sensors are in principle suitable for the purpose, because the sensor resonant frequency virtually does not depend on the interrogation configuration. The contactless generation of mechanical resonances in nonmagnetic microstructures to be used as sensors can be obtained by the interaction between an external static magnetic field and an AC current flowing either in the microstructure [1], or in a proximate coil [2, 3]. Magnetoelastic resonators can also be used [4]. We propose an alternative method that advantageously avoids the needs for static magnetic fields, electrical connections to the resonator, and specific material properties of the resonant structure except conductivity. The method exploits the Lorentz forces at the frequency  $2f_e$  generated in a conductive

resonator by an excitation magnetic field at  $f_e$ , and the modulation caused by the vibrations on a probing field at higher frequency  $f_p$ . The excitation and detection principles have been studied with the support of a mathematical model and FEM simulations. Experimentally the excitation and detection principles have been verified using two different sensing structures, in particular a doubly-clamped beam and a cantilever.

## II. THEORY

### A. The excitation principle

Fig. 1 shows a simplified schematic diagram of the principle of contactless electromagnetic excitation. A resonator with a conductive surface is placed in the region where a magnetic field is generated by a coil. The coil is composed of a central winding used for excitation and probing and two lateral windings for detection. As far as the excitation is considered, the central winding is driven by a sinusoidal time-varying current  $I_e(t)$  at frequency  $\omega_e$  to generate a sinusoidal magnetic field  $B_e(t)$ . Because of the axial symmetry of the configuration, the field  $B_e$  is made by a radial component  $B_{er}$  and a vertical component  $B_{ez}$ . The time variation of the flux of  $B_{ez}$  through the conductive surface of the resonator generates an electromotive force  $V_i(t)$ . The electromotive force is responsible for the circulation of an eddy current density  $J_i$  in the conductive layer. Due to the geometry,  $J_i$  has only in-plane component and the following expression can be derived,

$$J_i(t) = J_0(\omega_e) \sin(\omega_e t + \varphi) \quad (1)$$

where both the amplitude  $J_0$  and the phase  $\varphi$  are dependent on the electrical impedance  $Z(\omega) = |Z(\omega)| e^{j\varphi(\omega)}$  of the conductive layer. The eddy-current density interacts with the overall magnetic field and a Lorentz force per unit

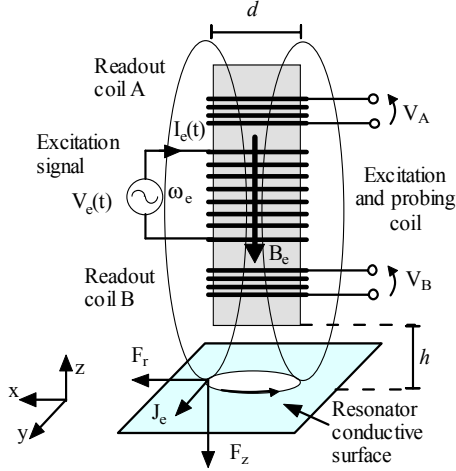


Figure 1. Schematic diagram of the excitation principle.

volume is generated which acts on the resonator. In particular, observing that the force in the  $z$  direction is given by the interaction of  $J_i$  with the component  $B_{er}$ , the following expression for the vertical force  $F_z$  can be derived

$$F_z = (1/2)J_0(\omega_e)B_{er}[\sin(\varphi) + \sin(2\omega_e t + \varphi)] \quad (2)$$

It can be observed that the force  $F_z$  is composed of a sinusoidal term at twice the excitation frequency  $\omega_e$ , proportional to the time-varying component of the external field plus a DC term dependent on the phase of the electrical impedance of the conductive layer. According to (2), to excite a vibration mode of a resonator at frequency  $\omega_r$ , the excitation coil must be driven at frequency  $\omega_e$  so that  $\omega_r = 2\omega_e$  [5].

### B. The detection principle

Fig. 2 shows a schematic diagram of the readout principle. In this case the resonator is supposed to vibrate in the  $z$  direction with a simple harmonic motion of peak amplitude  $Z_m$  at frequency  $2\omega_e$  caused by the excitation. The central winding is driven by a sinusoidal current  $I_p(t)$  at frequency  $\omega_p \gg \omega_e$  to generate a probing field  $B_p(t)$ . On the conductive surface of the resonator, the eddy-current density  $J_s$  is induced which is the sum of two contributions. The first contribution comes from the time-changing flux on the resonator caused by the vibrations. The second contribution comes from the time variation of the current  $I_p$ . In the studied configuration, it has been demonstrated that the first contribution can be neglected. The current density  $J_s$  generates a magnetic field  $B_s$  that can be sensed and used to measure the vibrations of the resonator. To this purpose, the sensing is performed by taking the differential voltage  $V_{AB}$  induced by the changing flux of  $B_s$  on the coils A and B. With the above assumptions on  $J_s$ , the differential voltage  $V_{AB}$  can be expressed as:

$$V_{AB} = 2A_s\omega_e Z_m \Delta k \sin(2\omega_e t) \cos(\omega_p t) + A_s\omega_p \Delta B_{0s} \sin(\omega_p t) \quad (3)$$

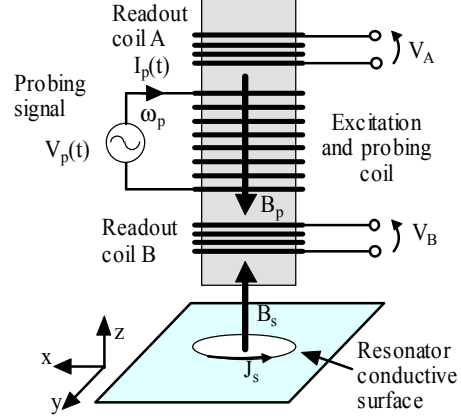


Figure 2. Schematic diagram of the readout principle.

where  $\Delta k$  and  $\Delta B_{0s}$  are two constants taking into account the dependence from the  $z$  coordinate of  $B_s$  and its derivative, and  $A_s$  is the area interested by  $B_s$ . Equation (3) predicts that in the readout signal  $V_{AB}$  spectral components at  $(\omega_p - 2\omega_e)$ ,  $(\omega_p + 2\omega_e)$  and  $\omega_p$  are present.

### III. SIMULATIONS

Simulations on the excitation and readout principles have been executed to verify the theoretical analysis. The simulations have been performed using Maxwell2D, commercialized by Ansoft, which permits to do electromagnetic analysis of two dimensional structures with cylindrical geometry. The geometry adopted to represent the real system is reported in Fig. 1. The core is made of linear ferromagnetic material with a relative magnetic permeability  $\mu_r = 1000$ , and with 5 mm diameter and 25 mm length. For computational reasons the central coil has been modelled as a single extended winding. The resonator is a titanium disk ( $\mu_r = 1.00018$  e  $\sigma = 2.1 \times 10^6$  S/m) with thickness of 100  $\mu\text{m}$  positioned under the ferrite core in central axial position. To verify the excitation principle, the central coil has been driven by a sinusoidal current  $I_e(t)$  at frequency 1 kHz and amplitude 100 A. The magnetic field  $B_e$  and the current density  $J_e$  induced onto the resonator have been derived. The simulation results of the components  $F_z$  and  $F_r$  of the Lorentz force are obtained considering the area under the ferrite core. Figs. 3a) and 3b) respectively show the diagrams of the radial component  $F_r$  and vertical component  $F_z$  at different values of the distance between the resonator plane and the ferrite core. The component  $F_r$  has a monotonic behaviour because both the induced current  $J_e$  and the component  $B_{ez}$  decrease with increasing the distance. On the other hand, the force component  $F_z$  presents a maximum, which for the adopted dimensions corresponds to a distance of 0.4 mm. This behaviour is justified considering that the amplitude of the current density  $J_e$  decreases monotonically when the distance increases, while the amplitude of the radial magnetic field  $B_{er}$  increases from a null value up to a maximum and then decreases.

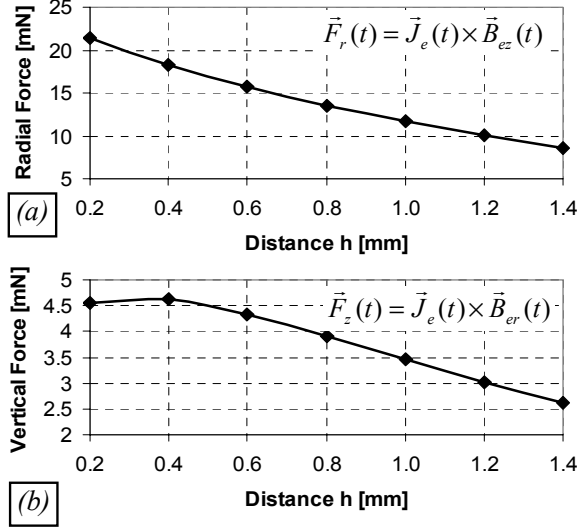


Figure 3. Simulation of the radial force  $F_r$  (a) vertical force  $F_z$  (b) versus the distance.

The readout principle, based on taking the flux difference between the two sensing coils, was also simulated. To this purpose, the central coil has been driven by a sinusoidal current  $I_p(t)$  at frequency 80 kHz and amplitude 100 A. The distance  $h$  between the resonator and the coil has been varied from 0.2 mm to 4 mm and the fluxes  $\Phi_A$  and  $\Phi_B$  through the coils A and B respectively have been calculated. Fig. 4 shows the trends of the quantity  $100(\Phi_A - \Phi_B)/\Phi_A$ , named Percentage Flux Difference (PFD), as a function of the distance  $h$  for different values of the coil diameter  $d$ . It can be observed that, for the adopted dimensions, a higher sensitivity in the readout can be achieved for distances  $h$  less than 3 mm. On the other hand, for a given distance  $h$  the PFD decreases for smaller values of the diameter  $d$  because the flux through the sensing coils also decreases.

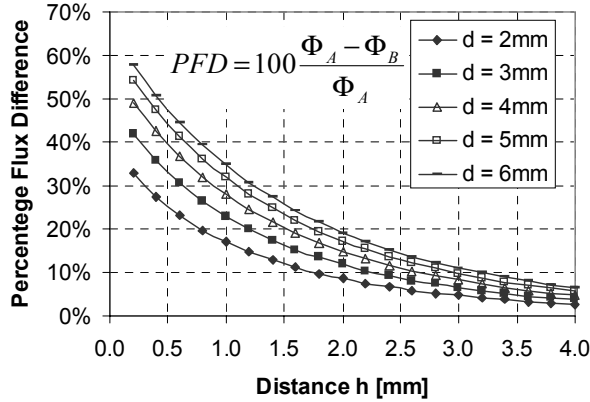


Figure 4. Simulation of the percentage flux difference versus distance for different diameters of the coil.

#### IV. EXPERIMENTAL RESULTS

Fig. 5 shows a schematic diagram of the experimental setup employed to carry out tests on metallic resonators. A previously developed optical system [6] has been used as a reference instrument to detect the vibrations of the resonators. The system provides swept-frequency excitation to the resonator under test by means of the excitation coil and detects the mechanical vibrations of the resonator by means of an optical triangulator composed of a laser diode and a position sensitive detector. The readout signal from the triangulator undergoes synchronous undersampling to derive the real and imaginary parts of the frequency response FR1 of the resonator. The intrinsic nonlinearity of the excitation principle requires a demodulation process at  $2f_e$ , performed by exploiting a suitable synchronization mechanism (X2) internal to the optical system. The processing is equivalent to a synchronous demodulation with lock-in detection. The measurement of the signal  $V_{AB}$  described in (3) is performed by a double synchronous demodulation process. A first demodulation at frequency  $f_p$  allows the recovery of signal at frequency  $2f_e$  proportional to the vibration amplitude of the resonator. A second demodulation process at  $2f_e$  is performed to measure the real and imaginary part of the frequency response FR2 of the resonator. Within the experimental errors, FR1 and FR2 show the same resonance value.

The inset of Fig. 6 shows the schematic drawing of the resonator employed at first to verify the excitation principle by using the optical readout only. A tunable resonator has been built by means of a 100  $\mu\text{m}$  thick clamped-clamped titanium beam with lateral dimensions of 17x1.4 mm mounted between two clamping holders. Titanium is characterized by Young's modulus  $E$  of  $105 \times 10^9$  Pa, mass density  $\rho$  of 4940 kg/m<sup>3</sup> and electrical conductivity  $\sigma$  of  $7.407 \times 10^5$  S/m. By applying an axial tension to the beam,

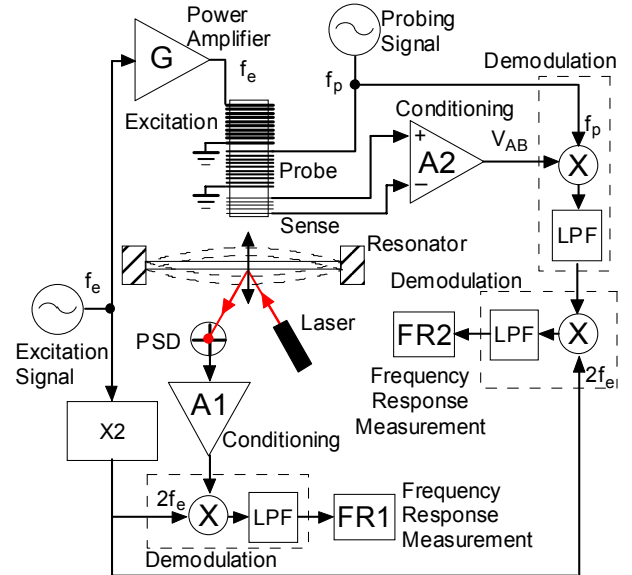


Figure 5. Schematic diagram of the experimental setup.

the resonance frequency can be changed. A measurement with no axial tension has been performed by driving the excitation coil in the range 950-1200 Hz with a current of 26 mA rms. In this condition, a resonance frequency of 2070 Hz has been detected corresponding to the first flexural mode of the beam, as shown in curve A of Fig. 6. In the same figure the curves labeled B, C, D show the frequency response of the resonator with three increasing axial tensions applied. As expected, when the axial tension of the beam is increased a corresponding frequency up-shift is observed.

The magnetic readout principle has been demonstrated by using an aluminum cantilever as the resonator. The cantilever has dimensions of 26x5x0.1 mm. Aluminum is characterized by Young's modulus  $E$  of  $69 \times 10^9$  Pa, mass density  $\rho$  2730 kg/m<sup>3</sup> and electrical conductivity  $\sigma$  of  $2.326 \times 10^7$  S/m. Preliminary, the cantilever has been characterized by means of the mechanical impulse response and a resonance frequency of 200 Hz has been estimated. Subsequently, the cantilever has been magnetically excited in the frequency range 95-110 Hz with a current in the coil of 35 mA. The frequency responses in the range 190-220 Hz were simultaneously measured by the magnetic readout method and the optical system taken as reference.

Fig. 7 shows the comparison between the obtained results. Both curves show a resonance frequency at about 202 Hz, with a remarkable agreement between the positions of the peaks, in accordance with the prediction of the impulse response.

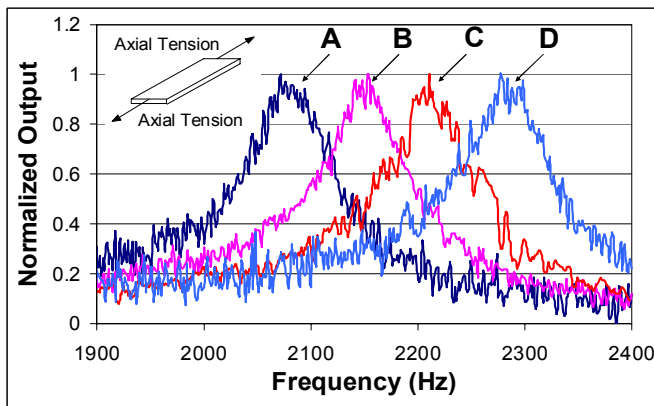


Figure 6. Frequency response measured by the optical readout system for applied axial tensions increasing from A to D. In the inset a schematic diagram of the doubly clamped resonator.

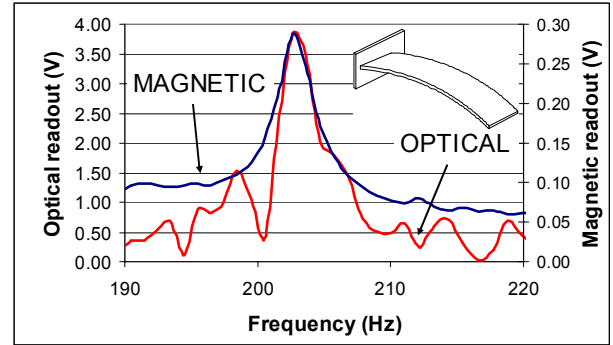


Figure 7. Comparison between the resonance measured by the magnetic readout method and the optical system as reference. In the inset a schematic diagram of the cantilever.

## V. CONCLUSIONS

In this work the possibility to induce vibrations in a contactless way on conductive and nonmagnetic structures by an external time-changing magnetic field has been proposed. The force acting on the structures is generated by the interaction between the eddy currents induced on the conductive surface by the time-varying magnetic field and the magnetic field itself. The theoretical predictions have been confirmed by FEM simulations and experimentally verified by tests carried out on millimeter-size resonators. As a second step, the contactless magnetic detection of the resonator vibrations has been demonstrated. The activity is now investigating the effect of the geometrical parameters of the resonant structures on the excitation and readout mechanism. Perspective application of the work is to apply the principle to microfabricated structures working as passive and robust sensing elements.

## REFERENCES

- [1] E. K. Reichel, B. Weiß, C. Riesch, A. Jachimowicz, B. Jakoby, "A novel micromachined liquid property sensor utilizing a doubly clamped vibrating beam" Proc. XX Eurosensors, Goteborg, Sweden, 17-20 September 2006.
- [2] F. Lucklum, P. Hauptmann, N. F. de Rooij, "Magnetic direct generation of acoustic resonance in silicon membranes", Meas. Sci. Technol., vol 17, p.719-726, 2006.
- [3] A. C. Stevenson, C. R. Lowe, "Magnetic-acoustic-resonator sensors (MARS): a new sensing methodology", Sensors and Actuators, vol. 72, p.32-37, 1999.
- [4] C. A. Grimes, D. Kouzoudis, C. Mungle, "Simultaneous measurement of liquid density and viscosity using remote query magnetoelastic sensors" Rev. Sci. Instrum., vol. 71, 10, p. 3822-3824, 2000.
- [5] C. De Angelis, V. Ferrari, D. Marioli, E. Sardini, M. Serpelloni, A. Taroni, "Magnetically induced oscillations on a conductive cantilever for resonant microsensors", Sensors and Actuators A, vol. 135, p. 197-202, 2007.
- [6] M. Baù, V. Ferrari, D. Marioli, A. Taroni, "Cost-effective system for the characterization of microstructures vibrating in out-of-plane modes", Sensors and Actuators A, 2007, in press.